

## Role of the Key Mutation in the Selective Binding of Avian and Human Influenza Hemagglutinin to Sialosides Revealed by Quantum-Mechanical Calculations

Toshihiko Sawada,<sup>\*,†,‡</sup> Dmitri G. Fedorov,<sup>†</sup> and Kazuo Kitaura<sup>†,§</sup>

*Nanosystem Research Institute, National Institute of Advanced Industrial Science and Technology (AIST), 1-1-1 Umezono, Tsukuba, Ibaraki 305-8568, Japan, Core Research for Evolutional Science and Technology (CREST), Japan Science and Technology Agency (JST), 4-1-8 Honcho, Kawaguchi, Saitama 332-0012, Japan, and Graduate School of Pharmaceutical Sciences, Kyoto University, Sakyo-ku, Kyoto 606-8501, Japan*

Received June 10, 2010; E-mail: sawada-t@aist.go.jp

**Abstract:** The selective binding between avian and human influenza A viral hemagglutinins (HA) subtype H3 and Neu5Ac $\alpha$ 2-3 and  $\alpha$ 2-6Gal (avian  $\alpha$ 2-3, human  $\alpha$ 2-6) is qualitatively rationalized by the fragment molecular orbital (FMO) method. We suggest a general model of analyzing protein–ligand interactions based on the electrostatic, polarization, dispersion, and desolvation components obtained from quantum-mechanical calculations at the MP2/6-31G(d) level with the polarizable continuum model of solvation. The favorable avian H3 (A/duck/Ukraine/1963)–avian  $\alpha$ 2-3 binding arises from the hydrophilic interaction between Gal-4 OH and side-chain NH<sub>2</sub>CO on Gln226, which is supported by the intermolecular hydrogen-bond network to the 1-COO group on Neu5Ac moiety. A substitution of Gln226Leu in the avian H3 HA1 domain increases the binding affinity to human  $\alpha$ 2-6 due to the Leu226...human  $\alpha$ 2-6 dispersion with a small entropic penalty during the complex formation. The remarkable human H3 (A/Aichi/2/1968)–human  $\alpha$ 2-6 binding is not governed by the Ser228-OH...OH-9 Neu5Ac hydrogen bond. These fragment-based chemical aspects can help design monovalent inhibitors of the influenza viral HA–sialoside binding and the simulation studies on the viral HAs–human  $\alpha$ 2-6 binding.

### Introduction

Research in biochemistry and molecular biology has elucidated the interaction between influenza A virion and host cell surface receptors, pointing out that viral spike glycoprotein hemagglutinin (HA) interacts with  $\alpha$ -sialoglycoproteins and  $\alpha$ -sialoglycolipids expressed on the target cell surface.<sup>1,2</sup> HA exists as a trimer of sialoside binding domain HA1 and membrane fusion domain HA2 with the shape of a cylindrical ectodomain of about 135 Å. The shallow sialoside binding site lies on the top of the three oblong HA1 domains, which recognizes the differences in the sialic acid species and the terminal sialic acid–galactose linkage on  $\alpha$ -sialooligosaccharide moieties.<sup>3</sup>

The HA1–sialoside binding is characterized as a lectin–carbohydrate interaction;<sup>4–7</sup> under the monovalent binding mode, the weak affinity with the dissociation constants  $K_D$  on the order

of micromolar to millimolar<sup>8–11</sup> is enhanced by the polyvalent interaction effect under the established binding assay conditions, for example, in the virion–sialoside bound erythrocyte,<sup>12,13</sup> bromelain-released HA–sialoglycoprotein bound plate,<sup>14</sup> virion–receptor bound plate,<sup>15–20</sup> and recombinant HA–glycan

- (8) Sauter, N. K.; Bednarski, M. D.; Wurzburg, B. A.; Hanson, J. E.; Whitesides, G. M.; Skehel, J. J.; Wiley, D. C. *Biochemistry* **1989**, *28*, 8388–8396.
- (9) Sauter, N. K.; Hanson, J. E.; Glick, G. D.; Brown, J. H.; Crowther, R. L.; Park, S. J.; Skehel, J. J.; Wiley, D. C. *Biochemistry* **1992**, *31*, 9609–9621.
- (10) Weinhold, E. G.; Knowles, J. R. *J. Am. Chem. Soc.* **1992**, *114*, 9270–9275.
- (11) Charych, D. H.; Nagy, J. O.; Spevak, W.; Bednarski, M. D. *Science* **1993**, *261*, 585–588.
- (12) Rogers, G. N.; Paulson, J. C. *Virology* **1983**, *127*, 361–373.
- (13) Suzuki, Y.; Nagao, Y.; Kato, H.; Matsumoto, M.; Nerome, K.; Nakajima, K.; Nobusawa, E. *J. Biol. Chem.* **1986**, *261*, 17057–17061.
- (14) Takemoto, D. K.; Skehel, J. J.; Wiley, D. C. *Virology* **1996**, *217*, 452–458.
- (15) Suzuki, Y.; Nakano, T.; Ito, T.; Watanabe, N.; Toda, Y.; Guiyun, X.; Suzuki, T.; Kobayashi, T.; Kimura, Y.; Yamada, A.; Sugawara, K.; Nishimura, H.; Kitame, F.; Nakamura, K.; Deya, E.; Kiso, M.; Hasegawa, A. *Virology* **1992**, *189*, 121–131.
- (16) Gambaryan, A. S.; Matrosovich, M. N. *J. Virol. Methods* **1992**, *39*, 111–123.
- (17) Critchley, P.; Dimmock, N. J. *Bioorg. Med. Chem.* **2004**, *12*, 2773–2780.
- (18) Yamada, S.; Suzuki, Y.; Suzuki, T.; Le, M. Q.; Nidom, C. A.; Sakai-Tagawa, Y.; Muramoto, Y.; Ito, M.; Kiso, M.; Horimoto, T.; Shinya, K.; Sawada, T.; Kiso, M.; Usui, T.; Murata, T.; Lin, Y.; Hay, A.; Haire, L. F.; Stevens, D. J.; Russell, R. J.; Gamblin, S. J.; Skehel, J. J.; Kawaoka, Y. *Nature* **2006**, *444*, 378–382.

<sup>†</sup> AIST.

<sup>‡</sup> CREST.

<sup>§</sup> Kyoto University.

- (1) Wang, Q.; Tao, Y. J., Eds. *Influenza: Molecular Virology*; Caister Academic Press: Norfolk, 2010.
- (2) Horimoto, T.; Kawaoka, Y. *Nat. Rev. Microbiol.* **2005**, *3*, 591–600.
- (3) Skehel, J. J.; Wiley, D. C. *Annu. Rev. Biochem.* **2000**, *69*, 531–569.
- (4) Dam, T. K.; Brewer, C. F. *Chem. Rev.* **2002**, *102*, 387–429.
- (5) Ohta, T.; Miura, N.; Fujitani, N.; Nakajima, F.; Niikura, K.; Sadamoto, R.; Guo, C.-T.; Suzuki, T.; Suzuki, Y.; Monde, K.; Nishimura, S.-I. *Angew. Chem., Int. Ed.* **2003**, *42*, 5186–5189.
- (6) Sharon, N.; Lis, H. *Lectins*, 2nd ed.; Springer: Dordrecht, 2007.
- (7) Dam, T. K.; Brewer, C. F. *Biochemistry* **2008**, *47*, 8470–8476.

array systems.<sup>21–25</sup> For the observed difference in the HA–sialosides binding under these polyvalent conditions with uniform density of sialoside receptors irrespective of their own chemical properties, an important inherent driving factor is given by the monovalent HA–monosialoside (1:1) binding in equilibrium solution.

Therefore, it is significant to study the HA–sialoside interaction in this model providing a basis for much more complex phenomena where dynamic (i.e., kinetic) factors may be important. Also, the 1:1 binding model directly pertains to the binding between soluble trivalent HA and monovalent sialoside, as was experimentally studied in the simple binding mode under equilibrium solution,<sup>8</sup> where the HA–sialoside binding is found not to be regulated by the sialoside homotropic allosteric effect.

Avian and human viral HAs differ in the binding affinities to  $\alpha$ -sialoside, and the specificity of the viral host range determination.<sup>26,27</sup> The avian viral HA subtype H3 HA1 domain involves Gln226 at the sialoside binding site, which binds to the avian-type sialoside receptor *N*-acetylneuraminic acid  $\alpha$ 2-3 galactose (Neu5Ac $\alpha$ 2-3Gal, avian  $\alpha$ 2-3) stronger than to the human-type receptor Neu5Ac $\alpha$ 2-6Gal (human  $\alpha$ 2-6).<sup>12,28,29</sup> On the other hand, human H3 contains Leu226 instead of Gln and preferentially binds to human  $\alpha$ 2-6.<sup>8,26–28</sup> An amino acid exchange from Gln to Leu at position 226 on H3 HA1 alters the binding specificity between avian  $\alpha$ 2-3 and human  $\alpha$ 2-6.<sup>8,30–32</sup> In the X-ray crystallographic structures of human and avian H3s in complex with sialoside, Gln/Leu at position 226 induces the characteristic orientation of Gal residue, while the common Neu5Ac residue location is almost unaffected.<sup>9,33–35</sup> This

qualitative observation should be related to the chemical mechanism of their specific sialoside binding. These findings are based on experimental evidence, but the key chemical factors in the recognition are not understood, although they are important for understanding the strong affinity of the pandemic human viral H1 subtype with Gln226 (H3 amino acid sequence numbering) to human  $\alpha$ 2-6.<sup>36–42</sup> Recent biotechnologies can test the affinity of miscellaneous HAs (e.g., wild type, recombinant HA, and reverse genetics products) binding to a various carbohydrate receptors, but their intrinsic picture in terms of biochemical interactions should be elucidated by *in silico* analysis. Molecular dynamic simulations<sup>19,43–46</sup> and free energy perturbation approach<sup>47</sup> have given a physical outline of the dynamic HA–sialoside interactions; however, more information is needed for residue interaction energies<sup>48</sup> of the HA–sialoside recognition.

The specific HA–sialoside association is governed by the binding free energy difference between the HA–avian  $\alpha$ 2-3 binding ( $\Delta G_{\text{bind},\alpha 2-3}$ ) and the HA–human  $\alpha$ 2-6 binding ( $\Delta G_{\text{bind},\alpha 2-6}$ ), which we analyze in the equilibrated monovalent HA–sialoside system by applying the *ab initio*-based fragment molecular orbital (FMO) method<sup>49</sup> with the polarizable continuum model (PCM)<sup>50–52</sup> at the second-order Møller–Plesset perturbation theory (MP2) with the 6-31G(d) basis set to reveal the role of key mutation in the preferred binding ( $\Delta G_{\text{bind},\alpha 2-3} < \Delta G_{\text{bind},\alpha 2-6}$ ) in the avian H3 HA1 domain–Neu5Ac $\alpha$ 2-3 and  $\alpha$ 2-6Gal complexes containing about 5000 atoms. General accuracy of FMO has been carefully evaluated in comparison to corresponding *ab initio* methods. For example, for the FMO-based

- (19) Auewarakul, P.; Suptawiwat, O.; Kongchanagul, A.; Sangma, C.; Suzuki, Y.; Ungchusak, K.; Louisirirotchanaikul, S.; Lertsamran, H.; Pooruk, P.; Thitithanyanont, A.; Pittayawonganon, C.; Guo, C.-T.; Hiramatsu, H.; Jampangern, W.; Chunsutthiwat, S.; Puthavathana, P. *J. Virol.* **2007**, *81*, 9950–9955.
- (20) Hidari, K. I. P. J.; Shimada, S.; Suzuki, Y.; Suzuki, T. *Glycoconjugate J.* **2007**, *24*, 583–590.
- (21) Stevens, J.; Blixt, O.; Paulson, J. C.; Wilson, I. A. *Nat. Rev. Microbiol.* **2006**, *4*, 857–864.
- (22) Kumari, K.; Gulati, S.; Smith, D. F.; Gulati, U.; Cummings, R. D.; Air, G. M. *Viol. J.* **2007**, *4*, 42–52.
- (23) Chandrasekaran, A.; Srinivasan, A.; Raman, R.; Viswanathan, K.; Raguram, S.; Tumpey, T. M.; Sasisekharan, V.; Sasisekharan, R. *Nat. Biotechnol.* **2008**, *26*, 107–113.
- (24) Stevens, J.; Blixt, O.; Chen, L.-M.; Donis, R. O.; Paulson, J. C.; Wilson, I. A. *J. Mol. Biol.* **2008**, *381*, 1382–1394.
- (25) A collaboration between the Consortium for Functional Glycomics (CFG) and Nature Publishing Group (NPG) is providing a comprehensive resource for functional glycomics research: <http://www.functionalglycomics.org>.
- (26) Suzuki, Y. *Biol. Pharm. Bull.* **2005**, *28*, 399–408.
- (27) Kawaoka, Y., Ed. *Influenza Virology Current Topics*; Caister Academic Press: Norfolk, 2006.
- (28) Connor, R. J.; Kawaoka, Y.; Webster, R. G.; Paulson, J. C. *Virology* **1994**, *205*, 17–23.
- (29) Matrosovich, M.; Tuzikov, A.; Bovin, N.; Gambaryan, A.; Klimov, A.; Castrucci, M. R.; Donatelli, I.; Kawaoka, Y. *J. Virol.* **2000**, *74*, 8502–8512.
- (30) Rogers, G. N.; Paulson, J. C.; Daniels, R. S.; Skehel, J. J.; Wilson, I. A.; Wiley, D. C. *Nature* **1983**, *304*, 76–78.
- (31) Ito, T.; Suzuki, Y.; Suzuki, T.; Takada, A.; Horimoto, T.; Wells, K.; Kida, H.; Otsuki, K.; Kiso, M.; Ishida, H.; Kawaoka, Y. *J. Virol.* **2000**, *74*, 9300–9305.
- (32) Rogers, G. N.; Daniels, R. S.; Skehel, J. J.; Wiley, D. C.; Wang, X. F.; Higa, H. H.; Paulson, J. C. *J. Biol. Chem.* **1985**, *260*, 7362–7367.
- (33) Weis, W.; Brown, J. H.; Cusack, S.; Paulson, J. C.; Skehel, J. J.; Wiley, D. C. *Nature* **1988**, *333*, 426–431.
- (34) Eisen, M. B.; Sabesan, S.; Skehel, J. J.; Wiely, D. C. *Virology* **1997**, *232*, 19–31.
- (35) Ha, Y.; Stevens, D. J.; Skehel, J. J.; Wiley, D. C. *Virology* **2003**, *309*, 209–218.
- (36) Ito, T.; Nelson, J.; Couceiro, S. S.; Kelm, S.; Baum, L. G.; Krauss, S.; Castrucci, M. R.; Donatelli, I.; Kida, H.; Paulson, J. C.; Webster, R. G.; Kawaoka, Y. *J. Virol.* **1998**, *72*, 7367–7373.
- (37) Gambelin, S. J.; Haire, L. F.; Russell, R. J.; Stevens, D. J.; Xiao, B.; Ha, Y.; Vasisht, N.; Steinhauer, D. A.; Daniels, R. S.; Elliot, A.; Wiley, D. C.; Skehel, J. J. *Science* **2004**, *303*, 1838–1842.
- (38) Soundararajan, V.; Tharakaraman, K.; Raman, R.; Raguram, S.; Shriver, Z.; Sasisekharan, V.; Sasisekharan, R. *Nat. Biotechnol.* **2009**, *27*, 510–513.
- (39) Childs, R. A.; Palma, A. S.; Wharton, S.; Matrosovich, T.; Liu, Y.; Chai, W.; Campanero-Rhodes, M. A.; Zhang, Y.; Eickmann, M.; Kiso, M.; Hay, A.; Matrosovich, M.; Feizi, T. *Nat. Biotechnol.* **2010**, *27*, 797–799.
- (40) Yang, H.; Carney, P.; Stevens, J. *PLoS Curr. Influenza* **2010**, RRN1152.
- (41) Xu, R.; Ekiert, D. C.; Krause, J. C.; Hai, R.; Crowe, J. E.; Wilson, I. A. *Science* **2010**, *328*, 357–360.
- (42) Zhang, W.; Qi, J. X.; Shi, Y.; Li, Q.; Gao, F.; Sun, Y. P.; Lu, X.; Lu, Q.; Vavricka, C. J.; Liu, D.; Yan, J. H.; Gao, G. F. *Protein Cell* **2010**, *1*, 459–467.
- (43) von der Lieth, C.-W.; Kozar, T. *J. Mol. Struct. (THEOCHEM)* **1996**, *368*, 213–222.
- (44) Kasson, P. M.; Ensign, D. L.; Pande, V. S. *J. Am. Chem. Soc.* **2009**, *131*, 11338–11340.
- (45) Newhouse, E. I.; Xu, D.; Markwick, P. R. L.; Amaro, R. E.; Pao, H. C.; Wu, K. J.; Alam, M.; McCammon, J. A.; Li, W. W. *J. Am. Chem. Soc.* **2009**, *131*, 17430–17442.
- (46) Xu, D.; Newhouse, E. I.; Amaro, R. E.; Pao, H. C.; Cheng, L. S.; Markwick, P. R. L.; McCammon, J. A.; Li, W. W.; Arzberger, P. W. *J. Mol. Biol.* **2009**, *387*, 465–491.
- (47) Das, P.; Li, J.; Royyuru, A. K.; Zhou, R. *J. Comput. Chem.* **2009**, *30*, 1654–1663.
- (48) Raha, K.; van der Vaart, A. J.; Riley, K. E.; Peters, M. B.; Westerhoff, L. M.; Kim, H.; Merz, K. M., Jr. *J. Am. Chem. Soc.* **2005**, *127*, 6583–6594.
- (49) Kitaura, K.; Ikeo, E.; Asada, T.; Nakano, T.; Uebayasi, M. *Chem. Phys. Lett.* **1999**, *313*, 701–706.
- (50) Fedorov, D. G.; Kitaura, K.; Li, H.; Jensen, J. H.; Gordon, M. S. *J. Comput. Chem.* **2006**, *27*, 976–985.
- (51) Barone, V.; Coss, M.; Tomasi, J. *J. Chem. Phys.* **1997**, *107*, 3210–3221.
- (52) Tomasi, J.; Mennucci, B.; Cammi, R. *Chem. Rev.* **2005**, *105*, 2999–3093.

polarizable continuum model (PCM) of solvation,<sup>50</sup> the solvation energies were reproduced within about 1 kcal/mol, whereas the general accuracy of PCM is discussed elsewhere.<sup>51,52</sup> Numerous applications of FMO (summarized in reviews<sup>53,54</sup>) have demonstrated its usefulness in applications to biochemical systems. More recently, He et al. have applied to protein folding the same FMO-MP2/PCM method as we used in this study.<sup>55</sup>

Our calculated binding energies qualitatively reproduced the available experimental order in vitro X-31 human virus strain H3 system.<sup>8</sup> The FMO-MP2/PCM method provides the components of the binding energy  $\Delta G_{\text{bind}}$ : the HA–sialoside intermolecular interaction stabilization in the gas phase, intramolecular internal energy destabilization of HA1 and sialoside in the complex relative to their free states, and desolvation penalty<sup>56</sup> for the HA–sialoside binding in the aqueous phase.

## Methods

**Preparation of Model Complexes.** We studied the A/duck/Ukraine/1963 strain (H3N8, abbreviation dkUkr/63) as avian H3, and the X-31 recombinant strain (H3N2, X-31) as human H3. Where “A” means influenza A virus, this avian virus was isolated from duck in Ukraine in 1963. The X-31 H3 was in accord with the corresponding H3 in A/Aichi/2/1968 (abbreviation Aichi2/68), which was labeled as strain number 2 isolated from human in Aichi/Japan in 1968. Starting from the corresponding X-ray crystallographic structures of the H3 trimer–sialoside complexes,<sup>9,33–35</sup> the models of avian and human H3 HA1 full domain monomers in complex with Neu5Ac $\alpha$ 2-3 and  $\alpha$ 2-6Gal disaccharides were taken from earlier work.<sup>57,58</sup> The modeling details are given here for completeness.

First, the avian H3 trimers in complex with geometry-determined Neu5Ac $\alpha$ 2-3 and  $\alpha$ 2-6Gal disaccharide moieties containing crystal water (PDB ID: 1MQM and 1MQN)<sup>35</sup> were geometry-optimized (energy-minimized) by utilizing the class II force field<sup>59</sup> implemented in the Discovery Studio program package.<sup>60</sup> The minimization was performed by utilizing the adopted basis Newton–Raphson algorithm with the generalized Born implicit solvent (solvent dielectric constant = 1, solvent generalized born dielectric constant = 80) until the rms gradient fell below  $1.0 \times 10^{-4}$  kcal mol<sup>-1</sup> Å<sup>-1</sup>. Next, cutting out the HA1 full domain monomer–Neu5Ac $\alpha$ –Gal complexes from the above energy minimum geometries gave the models for our computational study (Figure 1, left). Corresponding amino acid sequences and secondary structures are shown in Supporting Information Table S1.

The model of human H3 HA1 in complex with human Neu5Ac $\alpha$ 2-6Gal disaccharide was prepared by referring the crystal structure of the X-31 H3–human  $\alpha$ 2-6 sialopentasaccharide complex.<sup>34</sup> Starting from the crystal structure of X-31 H3 trimer with three Neu5Ac $\alpha$ 2-3Gal $\beta$ 1-4Glc (PDB ID: 1HGG),<sup>9</sup> we replaced the three sialosides with Neu5Ac $\alpha$ 2-6Gal disaccharides by means of superposing the common Neu5Ac $\alpha$  coordination. Next, we adapted the

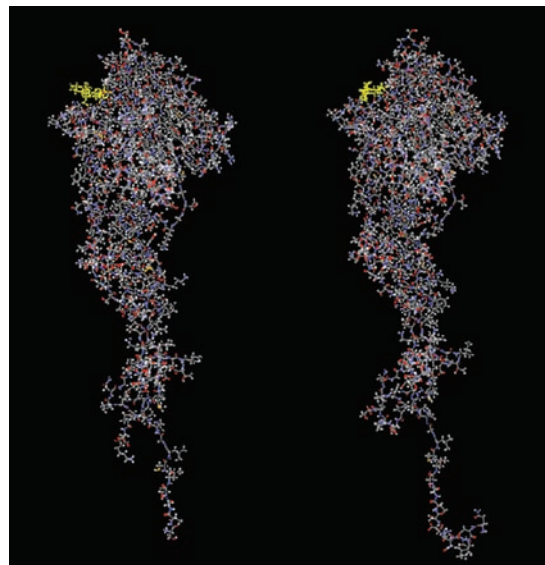


**Figure 1.** Optimized influenza viral H3 HA1 full domain in complex with Neu5Ac $\alpha$ 2-3 and  $\alpha$ 2-6Gal disaccharides. Left: Avian H3 HA1 (A/duck/Ukraine/1963 (dkUkr/63), H3N8, Ser9–Lys326) in complex with avian Neu5Ac $\alpha$ 2-3Gal (4932 atoms). Right: Human H3 HA1 (recombinant viral strain X-31, Gln1–Thr328) in complex with human Neu5Ac $\alpha$ 2-6Gal (5071 atoms). Neu5Ac $\alpha$ 2-3 and  $\alpha$ 2-6Gal disaccharides are shown in yellow. The amino acid sequences and the corresponding secondary structures are summarized in Table S1.

Leu226-induced conformation of the  $\alpha$ 2-6 glycoside bond with the following dihedral angles suggested by the crystal structure of X-31 H3–human  $\alpha$ 2-6 sialopentasaccharide complex:<sup>34</sup> Neu C<sup>1</sup>–C<sup>2</sup>–Gal O<sup>6</sup>–C<sup>6</sup> =  $-57^\circ$ , Neu C<sup>2</sup>–Gal O<sup>6</sup>–C<sup>6</sup>–C<sup>5</sup> =  $-154^\circ$ , and Gal O<sup>6</sup>–C<sup>6</sup>–C<sup>5</sup>–O<sup>5</sup> =  $62^\circ$ . Definitions for the dihedral angles are given in Supporting Information Figure S1. The X-31 H3 trimer–three Neu5Ac $\alpha$ 2-6Gal complex involving crystal water was prepared in the same way, yielding the model of human H3 HA1 full domain monomer–Neu5Ac $\alpha$ 2-6Gal complex (Figure 1, right).

The model of avian H3 Gln226Leu HA1 monomer in complex with human-type Neu5Ac $\alpha$ 2-6Gal was constructed by in silico point substitution from Gln226 to Leu in the crystal structure of avian H3 trimer–three Neu5Ac $\alpha$ 2-6Gal complex (PDB ID: 1MQN<sup>35</sup>). The side-chain orientation of Leu226 residue was suggested by the human H3 HA1 complex. The  $\alpha$ 2-6 bond conformation was changed to a Leu226-induced orientation with the above dihedral angles. The model involving crystal water was prepared in the same way, yielding the avian H3 Gln226Leu HA1–Neu5Ac $\alpha$ 2-6Gal complex.

Our initial models and their energy-minimized geometries should be reasonable to qualitatively discuss the H3 HA1–Neu5Ac $\alpha$ –Gal interactions. The Leu226-induced orientation of Gal residue on  $\alpha$ 2-6 receptors was observed in several crystallographic structures of influenza A viral HAs in complex with  $\alpha$ 2-6 sialopentasaccharide.<sup>33,34,61,62</sup> The Leu at position 226 (H3 amino acid sequence numbering) interacted with the hydrophobic 6-CH<sub>2</sub> group on Gal residue in  $\alpha$ 2-6 sialopentoside, while the terminal Neu5Ac residue was located in an almost same position regardless of the  $\alpha$ 2-3,  $\alpha$ 2-6, and HA subtypes. On the other hand, we confirmed the Gln/Leu226-dependent conformational behavior of Gal residue by performing classical molecular dynamics simulations under isobaric–isothermal (NPT) condition to the model of truncated H3 HA1 monomers in complex with Neu5Ac $\alpha$ 2-6 and  $\alpha$ 2-3Gal $\beta$ 1-

(53) Fedorov, D. G.; Kitaura, K. *J. Phys. Chem. A* **2007**, *111*, 6904–6914.

(54) Fedorov, D. G.; Kitaura, K., Eds. *The Fragment Molecular Orbital Method: Practical Applications to Large Molecular Systems*; CRC Press: Boca Raton, FL, 2009.

(55) He, X.; Fusti-Molnar, L.; Cui, G.; Merz, K. M., Jr. *J. Phys. Chem. B* **2009**, *113*, 5290–5300.

(56) Murata, K.; Fedorov, D. G.; Nakanishi, I.; Kitaura, K. *J. Phys. Chem. B* **2009**, *113*, 809–817.

(57) Sawada, T.; Hashimoto, T.; Nakano, H.; Suzuki, T.; Suzuki, Y.; Kawaoka, Y.; Ishida, H.; Kiso, M. *Biochem. Biophys. Res. Commun.* **2007**, *355*, 6–9.

(58) Sawada, T.; Hashimoto, T.; Tokiwa, H.; Suzuki, T.; Nakano, H.; Ishida, H.; Kiso, M.; Suzuki, Y. *Glycoconjugate J.* **2008**, *25*, 805–815.

(59) Maple, J. R.; Hwang, M.-J.; Jalkanen, K. J.; Stockfish, T. P.; Hagler, A. T. *J. Comput. Chem.* **1998**, *19*, 430–458.

(60) Discovery Studio 1.5.1, Accelrys, San Diego, CA.

(61) Ha, Y.; Stevens, D. J.; Skehel, J. J.; Wiley, D. C. *Proc. Natl. Acad. Sci. U.S.A.* **2001**, *98*, 11181–11186.

(62) Liu, J.; Stevens, D. J.; Haire, L. F.; Walker, P. A.; Coombs, P. J.; Russell, R. J.; Gamblin, S. J.; Skehel, J. J. *Proc. Natl. Acad. Sci. U.S.A.* **2009**, *106*, 17175–17180.

4Glc immersed in a periodic boundary TIP3P water box (Supporting Information, Appendix S1).

The forms of polar amino acid side-chains in the energy minimum HA–Neu5Ac $\alpha$ 2-3 and  $\alpha$ 2-6Gal complexes are as follows (HA1 domain region); all Arg formed  $\delta$ -guanidinium, all Lys formed  $\epsilon$ -ammonium, His17 and 75 in the human H3 complex formed neutral with N<sup>o</sup> proton and imidazolium, the other His formed neutral with N<sup>e</sup> proton in both avian and human H3 complexes, and all Asp and Glu formed carboxylate. Neu5Ac $\alpha$ –Gal receptor in the complex had negative charge from the carboxylate group at the C-1 position on Neu5Ac residue ( $pK_a = 2.5\text{--}2.9^{63}$ ) under the established HA–sialoside binding condition. The rms deviations of peptide backbone atoms C, C $\alpha$ , N between the crystal structures and their energy minimum structures were 0.329–0.374 Å in H3 trimer complexes and 0.323–0.370 Å in HA1 monomer full domains.

**Estimation of Binding Free Energies.** The free energy of binding  $\Delta G_{\text{bind}}$  of the avian and human viral H3 HA1 domain with Neu5Ac $\alpha$ 2-3 and  $\alpha$ 2-6Gal (Figure 1) is evaluated by the following expressions:

$$G_{\text{PCM}} = G_{\text{internal}} + G_{\text{es}} + G_{\text{cav}} + G_{\text{disp}} + G_{\text{rep}}$$

$$G_{\text{internal}} = E_{\text{gas}} + G_{\text{pold}}$$

$$\Delta G_{\text{PCM}} = G_{\text{PCM, complex}} - (G_{\text{PCM, H3 HA1}} + G_{\text{PCM, sialoside}})$$

$$\Delta S_{\text{solute}} = S_{\text{solute, complex}} - (S_{\text{solute, H3 HA1}} + S_{\text{solute, sialoside}})$$

$$\Delta G_{\text{bind}} = \Delta G_{\text{PCM}} - T\Delta S_{\text{solute}}$$

where the free energies  $G_{\text{PCM}}$  of the energy-minimized complexes, isolated H3 HA1s and Neu5Ac $\alpha$ 2-3 and  $\alpha$ 2-6Gal, were computed at 298 K at the FMO2-MP2/PCM[1(2)]/6-31G(d) level. The internal energy in solution  $G_{\text{internal}}$  is given by the sum of the gas-phase energy  $E_{\text{gas}}$  and the destabilization component of the solvent-induced polarization of the solute  $G_{\text{pold}}$ ,  $G_{\text{es}}$  is the solute–solvent electrostatic interaction energy ( $G_{\text{es}}$  includes the stabilization component of the solvent induced polarization of the solute, which is typically equal to about  $-2G_{\text{pold}}^{64,65}$ ),  $G_{\text{cav}}$  is the cavitation energy (describing the loss of the solvent free energy necessary to create a cavity for the solute),  $G_{\text{disp}}$  is the solute–solvent dispersion interaction energy, and  $G_{\text{rep}}$  is the solute–solvent exchange–repulsion interaction energy (i.e., the nonelectrostatic part of the interaction excluding the dispersion). The desolvation free energy  $\Delta G_{\text{solvation}}$  in the complex formation is given by  $\Delta G_{\text{solvation}} = \Delta G_{\text{pold}} + \Delta G_{\text{es}} + \Delta G_{\text{cav}} + \Delta G_{\text{disp}} + \Delta G_{\text{rep}}$ , where each component such as  $\Delta G_{\text{es}}$  is computed as the difference between the complex and free systems.  $\Delta G_{\text{solvation}}$  shows the change in the solvation free energy during the complex formation, when some surface of the interacting systems is desolvated. Thus,  $\Delta G_{\text{PCM}}$  in the H3 HA1–Neu5Ac $\alpha$ –Gal complex is equal to  $\Delta E_{\text{gas}} + \Delta G_{\text{solvation}}$ .

An important question is whether an explicit or implicit solvation model should be used. While the former is ultimately the right way, it requires extensive sampling to describe liquid state rather than clusters in gas phase. On the other hand, continuum models implicitly consider the liquid state, and their limitations are in the parametrization and the extent in which a particular solute and its active site can be described by continuum solvation. While continuum solvation models are extensively used, they do introduce errors in some cases where explicit solvent plays an important role in the active site and is particularly important.<sup>66–69</sup> However, for

our particular system, we find that in the crystallographic structures of H3–Neu5Ac $\alpha$ –Gal complexes, there are no crystallographically determined water molecules between active site amino acids and Neu5Ac $\alpha$ –Gal. In addition, according to classical molecular dynamics simulations we performed, weakly constrained water molecules support the active site–Neu5Ac interaction from the outer (bulk solvent) side. These constrained water molecules are often replaced by other waters in a bulk solvent phase (Supporting Information, Appendix 2). Thus, we conclude that the solvent effects can be adequately estimated by the continuum approach (PCM).

Our  $\Delta G_{\text{PCM}}$  analysis does not include the deformation penalty term<sup>70</sup> from conformational energy difference between free and bound states of HA1 and sialoside. We note that throughout this Article, single  $\Delta$  quantities always refer to the change of the respective values in the complex formation (values for the complex minus the two free systems), and  $\Delta\Delta$  values show the difference between two single  $\Delta$  quantities for two different complexes. Details of the FMO/PCM setup and fragmentation of the models are given in Supporting Information Appendix S3. All FMO calculations were carried out using the GAMESS package.<sup>71</sup>

The solute entropic contributions  $S_{\text{solute}}$  are calculated using the normal-mode analysis with the harmonic approximation at the molecular mechanics level, where  $S_{\text{solute}}$  is the sum of the rotational, translational, and vibrational entropies at 298 K under 1.0 atm in the gas phase with a distance-dependent dielectric to mimic solvent effects,  $\epsilon = 4r$  ( $r$  is interatomic distance).<sup>72,73</sup> We applied the PARM99 parameters<sup>74</sup> with Duan et al. phi psi torsion parameters<sup>75</sup> and amino94 charges<sup>74</sup> to H3 HA1s, and GLYCAM06e parameters<sup>76</sup> to Neu5Ac $\alpha$ 2-3 and  $\alpha$ 2-6Gal disaccharides. The models were optimized (energy-minimized) by conjugate gradient method with the dielectric constant  $\epsilon = 4r$  until the rms gradient became smaller than  $1.5 \times 10^{-4}$  kcal mol<sup>-1</sup> Å<sup>-1</sup>, without using a distance cutoff for nonbonded interactions. All 1.4 van der Waals and electrostatic interactions were scaled by 2.0 and 1.2, respectively. The normal modes of the energy minimum geometries were calculated with harmonic approximation at 298 K under 1.0 atm. The orders of  $T\Delta S_{\text{solute}}$  were moderately consistent with the reported  $T\Delta S_{\text{solute}}$  of the galectin1–oligosaccharide complexes,<sup>73</sup> which was one of the lectin–carbohydrate systems. The  $S_{\text{solute}}$  calculations were performed using sander and nmode programs in AMBER8 package.<sup>77</sup>

This is how we estimated  $T\Delta S_{\text{solute}}$ . On the other hand, the full values of the  $T\Delta S_{\text{solute}}$  term including the configurational (conformational and vibrational) entropy contributing to the deformation energy<sup>70</sup> are difficult to obtain as this requires extensive sampling for the large H3 trimer–sialoside models. Also, molecular dynamics

(63) Scheinthal, B. M.; Bettelheim, F. A. *Cabohydr. Res.* **1968**, *6*, 257–265.

(64) Fedorov, D. G.; Kitaura, K. *J. Comput. Chem.* **2007**, *28*, 222–237.

(65) Nakanishi, I.; Fedorov, D. G.; Kitaura, K. *Proteins: Struct., Funct., Bioinf.* **2007**, *68*, 145–158.

(66) Clarke, C.; Woods, R. J.; Gluska, J.; Cooper, A.; Nutley, M. A.; Boons, G. J. *J. Am. Chem. Soc.* **2001**, *123*, 12238–12247.

(67) Li, Z.; Lazaridis, T. *J. Phys. Chem. B* **2005**, *109*, 662–670.

(68) Abel, R.; Young, T.; Farid, R.; Berne, B. J.; Friesner, R. A. *J. Am. Chem. Soc.* **2008**, *130*, 2817–2831.

(69) Gauto, D. F.; Lella, S. D.; Guardia, C. M. A.; Estrin, D. A.; Martí, M. A. *J. Phys. Chem. B* **2009**, *113*, 8717–8724.

(70) Nemoto, T.; Fedorov, D. G.; Uebayasi, M.; Kanazawa, K.; Kitaura, K.; Komeiji, Y. *Comput. Biol. Chem.* **2005**, *29*, 434–439.

(71) (a) Schmidt, M. W.; Baldrige, K. K.; Boatz, J. A.; Elbert, S. T.; Gordon, M. S.; Jensen, J. H.; Koseki, S.; Matsunaga, N.; Nguyen, K. A.; Su, S.; Windus, T. L.; Dupuis, M.; Montgomery, J. A., Jr. *J. Comput. Chem.* **1993**, *14*, 1347–1363. (b) Fedorov, D. G.; Kitaura, K. *J. Chem. Phys.* **2004**, *120*, 6832–6840.

(72) Chong, L. T.; Duan, Y.; Wang, L.; Massova, I.; Kollman, P. A. *Proc. Natl. Acad. Sci. U.S.A.* **1999**, *96*, 14330–14335.

(73) Ford, M. G.; Weimar, T.; Köhli, T.; Woods, R. J. *Proteins: Struct., Funct., Genet.* **2003**, *53*, 229–240.

(74) Cornell, W. D.; Cieplak, P.; Bayly, C. I.; Gould, I. R.; Merz, K. M.; Ferguson, D. M.; Spellmeyer, D. C.; Fox, T.; Caldwell, J. W.; Kollman, P. A. *J. Am. Chem. Soc.* **1995**, *117*, 5179–5197.

(75) Duan, Y.; Wu, C.; Chowdhury, S.; Lee, M. C.; Xiong, G.; Zhang, W.; Yang, R.; Cieplak, P.; Luo, R.; Lee, T.; Caldwell, J.; Wang, J.; Kollman, P. *J. Comput. Chem.* **2003**, *24*, 1999–2012.

(76) Kirschner, K. N.; Yongye, A. B.; Tschampel, S. M.; González-Outeiriño, J.; Daniels, C. R.; Foley, B. L.; Woods, R. J. *J. Comput. Chem.* **2008**, *29*, 622–655. GLYCAM06e is available from [http://glycam.ccr.cornell.edu/documents/gl\\_params.jsp](http://glycam.ccr.cornell.edu/documents/gl_params.jsp).

**Table 1.** Binding Energy  $\Delta G_{\text{bind}}$  and Its Components (See Text) in kcal/mol for the Avian and Human H3 HA1–Neu5Ac $\alpha$ 2-3 and  $\alpha$ 2-6Gal Complexes at the FMO2-MP2/PCM[1(2)]/6-31G(d) Level

entry	components of $\Delta G_{\text{bind}}$	avian H3/avian $\alpha$ 2-3	avian H3/human $\alpha$ 2-6	avian H3 Gln226Leu/human $\alpha$ 2-6	human H3/human $\alpha$ 2-6
1	$\Delta E_{\text{gas}}$	−237.1	−226.0	−214.6	−230.3
2	$\Delta G_{\text{pold}}$	−34.5	−28.4	−27.3	−28.2
3	$\Delta G_{\text{internal}}$	−271.6	−254.4	−241.9	−258.5
4	$\Delta G_{\text{es}}$	210.7	199.7	191.4	200.3
5	$\Delta G_{\text{cav}}^a$	−5.5	−6.1	−5.1	−3.1
6	$\Delta G_{\text{disp}}$	50.1	47.4	47.7	53.5
7	$\Delta G_{\text{rep}}$	−12.4	−12.3	−12.6	−13.5
8	$\Delta G_{\text{solvation}}^b$	208.4	200.3	194.1	209.0
9	$\Delta G_{\text{PCM}}^c$	−28.7	−25.7	−20.5	−21.3
10	$-T\Delta S_{\text{solute}}^a$	28.2	31.0	20.0	17.0
11	$\Delta G_{\text{bind}}^d$	−0.5	5.3	−0.5	−4.3

<sup>a</sup> 1.0 atm, 298 K. <sup>b</sup> Sum of entries 2 and 4–7. <sup>c</sup> Sum of entries 1 and 8 (entry 8 is the sum of entries 3–7). <sup>d</sup> Sum of entries 9 and 10.

simulation of the isolated HA1 domain monomer with explicit waters does not provide a reasonable  $T\Delta S_{\text{solute}}$ , because the tail of the HA1 domain fluctuates unnaturally, and the inner hydrophobic surface on HA1 monomer buried under the original HA1–HA2 trimerization behaves abnormally; therefore, one has to consider very large trimer systems, which requires very considerable computational resources.<sup>45,46</sup> In addition, in the framework of our focus on the effect of the mutation, the relative contribution of the full conformational entropy can be expected to be relatively small, and thus we did not perform the normal mode or essential dynamics analysis.<sup>78</sup> We note that in the normal-mode analysis with harmonic approximation,<sup>79–81</sup> the low frequency vibrational modes are often affected by the unharmonicity.<sup>80,82</sup> Finally, although the configurational entropic changes are hard to calculate, the ideal-gas solute translational and rotational entropic penalties during the complex formation can be overestimated in a large biomolecule–small ligand complex system.<sup>83–85</sup> These effects are diminished when one compares the differences in the free binding energies, that is, when comparing the effects of a mutation, which is the focus of this work.

## Results and Discussion

### Origin of the Preferential Avian H3–Avian $\alpha$ 2-3 Binding.

According to  $\Delta G_{\text{bind}}$  summarized in Table 1 (entry 11, −0.5 vs 5.3 kcal/mol), our approach estimates that avian H3 HA1 binds to avian  $\alpha$ 2-3 stronger than to human  $\alpha$ 2-6. This  $\Delta G_{\text{bind},\alpha 2-3}$  is comprised of the favorable  $\Delta E_{\text{gas}}$  with a larger desolvation penalty  $\Delta G_{\text{solvation}}$  (resulting in the exothermic  $\Delta G_{\text{PCM}}$ ,  $\Delta G_{\text{PCM}} = \Delta E_{\text{gas}} + \Delta G_{\text{solvation}}$ ) and a smaller  $T\Delta S_{\text{solute}}$  penalty (entries 1, 8–10).  $\Delta E_{\text{gas}}$  describes the intermolecular HA–sialoside interaction stabilization in the complex and the destabilization of the intramolecular internal energy of isolated H3 and sialosides. The  $\Delta E_{\text{gas}}$  benefit in the two avian H3 HA1–sialoside

complexes is compensated by the desolvation penalty  $\Delta G_{\text{solvation}}$  in the aqueous phase (Table 1, entries 1 and 8). In particular, the electrostatic term  $\Delta G_{\text{es}}$  contributes to  $\Delta G_{\text{solvation}}$  (entry 4) because many intermolecular hydrogen bonds form in the avian H3–sialoside complexes.<sup>58</sup> Comparing the avian H3 complexes, one can see that the avian H3–avian  $\alpha$ 2-3 binding suffers a 11.0 kcal/mol larger  $\Delta G_{\text{es}}$  penalty than does human  $\alpha$ 2-6. The larger  $\Delta G_{\text{es}}$  contains the desolvation penalty due to the formation of the intermolecular hydrogen-bond network around Gln226 and avian Neu5Ac $\alpha$ 2-3Gal.<sup>58</sup>

The intermolecular hydrogen-bond stabilization includes the dispersion contribution as well. The H3 HA1–sialoside complexes are also stabilized by the intermolecular dispersion such as Trp153-indole...CH<sub>3</sub>CONH-5 Neu5Ac and Leu194...CH-7/CH<sub>2</sub>-9 Neu5Ac. Table 1 entry 6 shows that the solute–solvent dispersion penalty  $\Delta G_{\text{disp}}$  in the complex formation is about 1/4 of  $\Delta G_{\text{es}}$ .  $\Delta G_{\text{disp}}$  is 2.7 kcal/mol larger in the case of avian H3–avian  $\alpha$ 2-3. On the other hand, several  $\Delta G_{\text{solvation}}$  components promote the H3–sialoside binding such as  $\Delta G_{\text{pold}}$ ,  $\Delta G_{\text{cav}}$ , and  $\Delta G_{\text{rep}}$  (entries 2,5,7). The solvent-induced solute polarization in the aqueous phase generally destabilizes the solute internal energy.<sup>86,87</sup> Thus, Table 1 entry 2 suggests that the decrease of the destabilization component  $G_{\text{pold}}$  of the polarization via the complex formation gives the −34.5 kcal/mol advantage in the avian H3–avian  $\alpha$ 2-3 complex, and the −28.4 kcal/mol advantage in the avian H3–human  $\alpha$ 2-6 complex. The solute cavity surface is decreased by the H3–sialoside association giving  $\Delta G_{\text{cav}}$  of −6.1 to −5.1 kcal/mol in the avian H3 complexes in both avian  $\alpha$ 2-3 and human  $\alpha$ 2-6 (entry 5). The decrease of the solute cavity surface monotonously reduces the solute–solvent repulsion  $\Delta G_{\text{rep}}$ , resulting in the favorable  $\Delta G_{\text{rep}}$  of −12.4 to −12.3 kcal/mol (entry 7).

With the above components of the solvation free energy, the avian H3 (A/duck/Ukraine/1963, dkUkr/63)–avian  $\alpha$ 2-3 binding has a more favorable  $\Delta G_{\text{PCM}}$  by −3.0 kcal/mol than in the avian H3–human  $\alpha$ 2-6 binding (entry 9). The  $\Delta G_{\text{PCM}}$  benefit is predominantly caused by the  $\Delta G_{\text{internal}}$  difference of −17.2 kcal/mol,  $\Delta G_{\text{es}}$  difference of +11.0 kcal/mol, and  $\Delta G_{\text{disp}}$  difference of +2.7 kcal/mol. Finally, with a small  $T\Delta S_{\text{solute}}$  penalty in the avian  $\alpha$ 2-3 binding (entry 10), the dkUkr/63–avian  $\alpha$ 2-3 complex obtains an advantage of −5.8 kcal/mol free energy relative to the dkUkr/63–human  $\alpha$ 2-6 binding (entry 11).

It is difficult to compare directly our results to experiment due to no available titration data for the interaction between

- (77) Case, D. A.; Darden, T. A.; Cheatham, T. E., III; Simmerling, C. L.; Wang, J.; Duke, R. E.; Luo, R.; Merz, K. M.; Wang, B.; Pearlman, D. A.; Crowley, M.; Brozell, S.; Tsui, V.; Gohlke, H.; Mongan, J.; Hornak, V.; Cui, G.; Beroza, P.; Schafmeister, C.; Caldwell, J. W.; Ross, W. S.; Kollman, P. A. *AMBER 8*; University of California: San Francisco, CA, 2004.
- (78) Hayward, S.; de Groot, B. L. Normal Modes and Essential Dynamics. In *Molecular Modeling of Proteins*; Methods in Molecular Biology 443; Kukol, A., Ed.; Humana Press: Totowa, NJ, 2008; pp 89–106.
- (79) Grünberg, R.; Nilges, M.; Leckner, J. *Structure* **2006**, *14*, 683–693.
- (80) Numata, J.; Wan, M.; Knapp, E.-W. *Genome Inf.* **2007**, *18*, 192–205.
- (81) Chang, C.-A.; Chen, W.; Gilson, M. K. *Proc. Natl. Acad. Sci. U.S.A.* **2007**, *104*, 1534–1539.
- (82) Baron, R.; van Gunsteren, W. F.; Hünenberger, P. H. *Trends Phys. Chem.* **2006**, *11*, 87–122.
- (83) Lazaridis, T. *Curr. Org. Chem.* **2002**, *6*, 1319–1332.
- (84) Murray, C. W.; Verdonk, M. L. *J. Comput.-Aided Mol. Des.* **2002**, *16*, 741–753.
- (85) Irudayam, S. J.; Henchman, R. H. *J. Phys. Chem. B* **2009**, *113*, 5871–5884.

- (86) Komeiji, Y.; Ishida, T.; Fedorov, D. G.; Kitaura, K. *J. Comput. Chem.* **2007**, *28*, 1750–1762.
- (87) Sawada, T.; Fedorov, D. G.; Kitaura, K. *Int. J. Quantum Chem.* **2009**, *109*, 2033–2045.

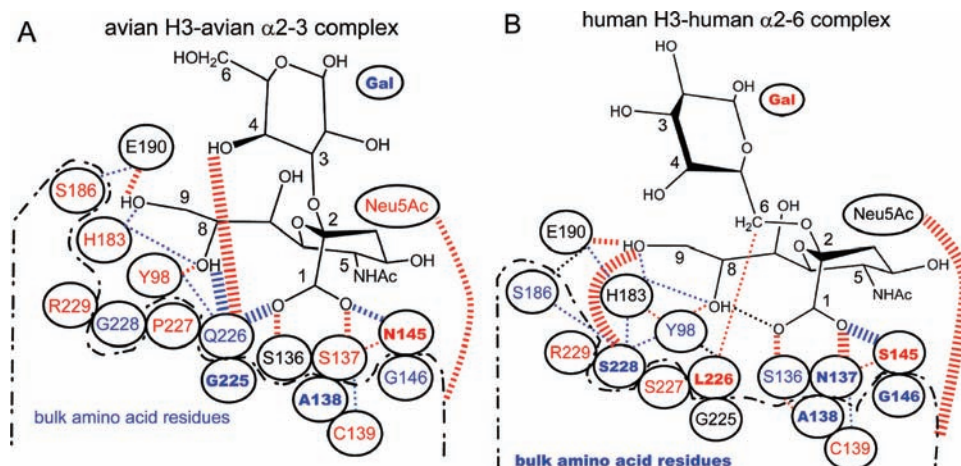


**Figure 2.** Symbolic representation of the gas-phase components of H3 HA1–Neu5Ac $\alpha$ 2-3 and  $\alpha$ 2-6Gal interactions. (A) Avian H3–avian  $\alpha$ 2-3 complex C1 relative to the avian H3–human  $\alpha$ 2-6 complex C2; (B) human H3–human  $\alpha$ 2-6 complex C3 relative to the avian H3–Gln226Leu–human  $\alpha$ 2-6 complex C4. Red dotted lines, the interactions favor C1 and C3; blue dotted lines, the interactions favor C2 and C4; black dotted lines in (B), no differences of the interaction energy contributions between the complexes. Wide lines,  $\sim$ 10 kcal/mol; medium lines, 2–10 kcal/mol; narrow lines, 0.5–2 kcal/mol. Red residues, the internal energies favor C1 and C3; blue residues, the internal energies favor C2 and C4; black residues, no difference in the internal energy contributions between the complexes. Bold type,  $\sim$ 1.0 kcal/mol in (A) and  $\sim$ 1.4 kcal/mol in (B); normal type, 0.4–1.0 kcal/mol in (A) and 0.5–1.4 kcal/mol in (B). Details are shown in Tables S4–S6 for (A) and Tables S10–S12 for (B).

isolated-dkUkr/63 HA and sialosides under equilibrium monovalent condition. However, the difference in the two  $\Delta G_{\text{bind}}$  values of  $-5.8$  kcal/mol (Table 1, entry 11) is of an order similar to the experimental binding free energy difference of  $-3.1$  to  $-1.9$  kcal/mol between the dkUkr/1/63 virion (polyvalent HA)–Neu5Ac $\alpha$ 2-3Gal $\beta$ 1-4Glc complex and the corresponding Neu5Ac $\alpha$ 2-6Gal $\beta$ 1-4Glc complex at  $4$  °C.<sup>16</sup> The experimental order was evaluated as a difference of the inhibition abilities of Neu5Ac $\alpha$ 2-3Gal $\beta$ 1-4Glc and Neu5Ac $\alpha$ 2-6Gal $\beta$ 1-4Glc toward the binding between solid phase-attached virion and peroxidase-labeled fetuin,<sup>16</sup> where fetuin had three Asn-linked sialoglycans. We note that an exact agreement to our results should not be expected due to both differences in the system; in the polyvalent system, mass-transport limitation strongly influences the effective binding free energy.

Next, we demonstrate that  $\Delta E_{\text{gas}}$  components analysis clarifies the origin of specific avian H3–avian  $\alpha$ 2-3 binding because the  $\Delta G_{\text{PCM}}$  advantage in the avian  $\alpha$ 2-3 binding is not offset by the  $T\Delta S_{\text{solute}}$  contribution (Table 1, entries 9 and 10). According to the comparison of the  $\Delta E_{\text{gas}}$  components (Figure 2A and Tables S4–S6), the preferential avian H3 (dkUkr/63)–avian  $\alpha$ 2-3 binding arises from the following three factors: (1) the larger intermolecular stabilization by the Gal4-OH $\cdots$ Gln226 interaction, (2) the smaller destabilization of the intermolecular hydrogen-bond network between 1-COO Neu5Ac and 4 amino acid residues Gln226, Ser136, Ser137, and Asn145, and (3) the favorable long-range electrostatic stabilization between avian  $\alpha$ 2-3 and bulk amino acids.

The former two factors compensate each other, resulting in the marked avian  $\alpha$ 2-3 recognition. Therefore, the hydrophilic recognition for 1-COO Neu5Ac is significant for the selective avian H3–avian  $\alpha$ 2-3 binding despite the relatively weaker stability than in the avian H3–human  $\alpha$ 2-6 binding. The suggestion is consistent with the known experimental results. A/duck/Hokkaido/7/1982 (H3N8, dkHok7/82) HA1 underwent a Gly228Ser substitution (almost all human H3 strains have Ser228) with Gln226 intact and an exchange between Ser and Asn at the positions 137 and 145, and retained the specific avian  $\alpha$ 2-3 binding.<sup>29</sup> The Ser137–Asn145 exchange can take place due to keeping the hydrogen-bond network for 1-COO Neu5Ac

(Figure 3); indeed major avian H3 strains following 1963 contained the exchange.<sup>28,29</sup>

As shown in Figure 3A, in the dkUkr/63 HA1–sialoside complex, the COO group in the Neu5Ac residue forms the intermolecular hydrogen-bond network with Gln226–CONH<sub>2</sub>, Ser137–NH–OH, Ser136–OH, and Asn145–CONH<sub>2</sub> on the sialoside binding site (Gln226 is not shown). This interaction network enables the wide-range recognition for 1-COO Neu5Ac. Comparing Figure 3A–C suggests that an exchange between Ser and Asn at the positions 137 and 145 maintains the wide-range 1-COO recognition for both  $\alpha$ 2-3 and  $\alpha$ 2-6 complexes. Keeping this interaction manner, the additional Gal 4-OH $\cdots$ H<sub>2</sub>NOC–Gln226 interaction governs the remarkable H3–avian  $\alpha$ 2-3 binding. Actually, a substitution of Leu226Gln on human H3 HA1 critically changes its binding specificity from human  $\alpha$ 2-6 to avian  $\alpha$ 2-3.<sup>29–31</sup>

It is difficult to link our third suggested factor to available experimental evidence. This issue is significant because the surface antigenic area including the Asn-glycosylation site in HA1, where amino acids are often substituted, lies around the sialoside binding site.<sup>88–90</sup> We now analyze it in detail, in particular amino acids within 13 Å radius<sup>91</sup> surrounding sialopentasaccharide moiety under the model complex of HA with natural receptor  $\alpha$ 2,6-sialylparagloboside.<sup>12,13,92</sup>

Our  $\Delta E_{\text{gas}}$  components analysis can be used to infer the following about the origin of the specific avian H3–avian  $\alpha$ 2-3 binding: (1) there is no relationship between Pro/Ser at position 227 and the distinctive avian H3–avian  $\alpha$ 2-3 binding; and (2) Gly228 does not govern the specific avian H3–avian  $\alpha$ 2-3 binding; actually the Gly228Arg substitution suitably changes

(88) Ohuchi, M.; Ohuchi, R.; Feldmann, A.; Klenk, H.-D. *J. Virol.* **1997**, *71*, 8377–8384.

(89) Romanova, J.; Katinger, D.; Ferko, B.; Voglauer, R.; Mochalova, L.; Bovin, N.; Lim, W.; Katinger, H.; Egorov, A. *Virology* **2003**, *307*, 90–97.

(90) Kasson, P. M.; Pande, V. S. *Biophys. J.* **2008**, *95*, L48–L50.

(91) Sawada, T.; Hashimoto, T.; Tokiwa, H.; Suzuki, T.; Nakano, H.; Ishida, H.; Kiso, M.; Suzuki, Y. *J. Mol. Genet. Med.* **2009**, *3*, 133–142.

(92) Suzuki, Y.; Kato, H.; Naeve, C. W.; Webster, R. G. *J. Virol.* **1989**, *63*, 4298–4302.

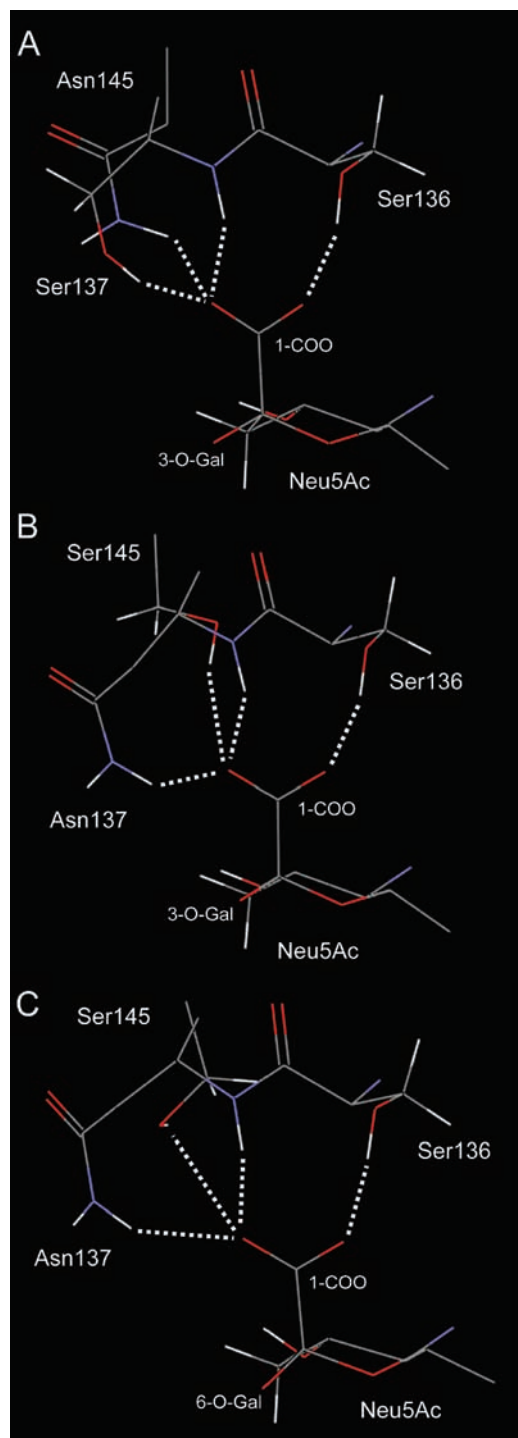


**Figure 3.** Hydrophilic recognition of 1-COO group on Neu5Ac by the amino acid residues at positions 136, 137, and 145: (A) avian H3 (dkUkr/63, Ser137, Asn145)–avian  $\alpha$ 2-3 complex; (B) model of avian H3 (Ser137Asn, Asn145Ser) in complex with avian  $\alpha$ 2-3; (C) human H3 (Aichi2/68, Asn137, Ser145)–human  $\alpha$ 2-6 complex. Complexes (A) and (C) are studied in this work. Complex (B) (found in major avian H3 strains following 1963) was prepared from complex (A) by in silico substitutions.

the hydrophilic recognition for 1-COO Neu5Ac to maintain the specific avian H3–avian  $\alpha$ 2-3 binding.

According to the component analysis of the  $\Delta E_{\text{gas}}$  difference (Figure 2A), Pro227 does not contribute to the favorable avian H3–avian  $\alpha$ 2-3 binding; in other words, there is no reason why avian H3 HA1 has Pro227. Thus, the known major avian H3

strains isolated following 1963 underwent the Pro227Ser substitution on HA1 that maintained or enhanced the binding affinity to avian  $\alpha$ 2-3.<sup>29</sup> Major human H3 strains also have Ser227 with their specific human  $\alpha$ 2-6 binding affinities. The Gly228 does not govern the selective avian H3–avian  $\alpha$ 2-3 binding as well (Figure 2A). We suppose that Gly228 only adjusts itself to the shape of the sialoside binding site by utilizing its own small size. In the previous experiment, dkHok7/82 had Gln226 and Ser228 in the HA1 domain whose specificity to avian  $\alpha$ 2-3 was preserved<sup>28,29</sup> because the Ser228 was of about the same size as Gly228; moreover, the OH group in Ser228 easily formed a new intermolecular hydrogen bond with OH-9 in Neu5Ac. Indeed, the Ser228-OH $\cdots$ OH-9 Neu5Ac interaction is observed in the human H3–sialoside complex as described in the next section.

Unexpectedly, depending on the unique condition, the Gly228 on avian H3 HA1 is substituted to a bulky Arg while keeping the specific avian  $\alpha$ 2-3 binding (Figure 4). Indeed, A/mallard/New York/6874/1978 (H3N2, maNY6874/78) underwent the substitutions Gly228Arg, Ser137Gly, and Pro227Ser with conservations of Ser136 and Asn145 (based on the dkUkr/63 amino acid sequence),<sup>29,31</sup> besides A/duck/Hokkaido/8/1980 (H3N8, dkHok8/80) had the substitutions Gly228Arg, Ser137Lys, and Asn145Ser.<sup>29</sup> In their molecular recognitions of avian  $\alpha$ 2-3, the interaction network between amino acids and Neu5Ac 1-COO was optimized by the amino acid substitutions at 137 and 145 to soften a bulky Arg228 $\cdots$ Neu5Ac interaction. The Gly228Arg substitution in the avian  $\alpha$ 2-3 complex can provide a new intermolecular hydrogen-bond network between Arg228  $\delta$ -guanidinium, OH-9 Neu5Ac, 4-OH Gal, H<sub>2</sub>NOC–Gln226, and OOC–Glu190 (Figure 4A). At the same time, the Arg228 $\cdots$ avian  $\alpha$ 2-3 hydrogen bond causes steric repulsion instability around the bulky Arg228 in the sialoside binding site.

To soften the Arg228 repulsion, the Neu5Ac moiety prefers shifting outside from the 1-COO Neu5Ac recognition site. When the Neu5Ac is thus shifted, it can possibly form a hydrogen bond between Ser137-OH and outer-edge OOC-1 on Neu5Ac with the Asn145 intact. Actually, maNY6874/78 was insensitive to the change from Ser137 to Gly (Figure 4B), keeping the specific avian  $\alpha$ 2-3 binding. dkHok8/80 underwent the Gly228Arg substitution similar to maNY6874/78; moreover, dkHok8/80 had Ser137Lys and Asn145Ser substitutions (based on dkUkr/63 amino acid sequence).<sup>29</sup> When the Asn145 mutated to Ser bearing the shorter hydrophilic side-chain –CH<sub>2</sub>OH, the Ser137Gly substitution probably did not occur due to insufficient 1-COO recognition. Instead,  $\epsilon$ -ammonium on Lys137 can form new hydrogen bonds with 1-COO Neu5Ac and 3-O-Gal (Figure 4C).

Finally, we mention the role of Gal residue on Neu5Ac $\alpha$ –Gal receptors in the free energy contribution. The interaction energy contribution (enthalpy) of Gal residue is large in the avian Gln226 H3–avian Neu5Ac $\alpha$ 2-3Gal complex stabilized by the intermolecular hydrogen-bond network around Gln226 with Gal 4-OH, Neu5Ac 1-COO, and Neu5Ac 8-OH. Actually, the other OH groups and hydrophobic surface constructed by C<sup>1</sup>–H, C<sup>3</sup>–H, C<sup>4</sup>–H, and C<sup>5</sup>–H on both Gal residues in Neu5Ac $\alpha$ 2-3 and  $\alpha$ 2-6Gal do not interact specifically with the active site amino acids on avian H3 HA1. Instead of this enthalpic advantage, the avian H3–avian  $\alpha$ 2-3 complex may suffer a larger torsional entropic penalty of the Neu5Ac $\alpha$ 2-3Gal glycosyl bond. However, the difference of torsional entropic penalties in the avian H3 complexes between Neu5Ac $\alpha$ 2-3Gal receptor and Neu5Ac $\alpha$ 2-6Gal receptor can be within 1 kcal/mol on the

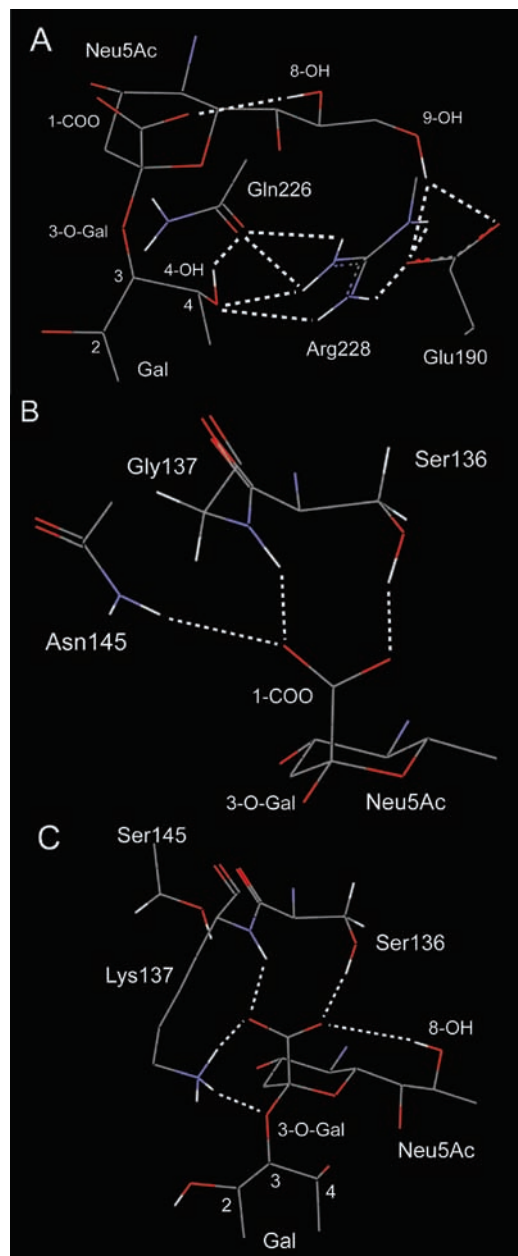


**Figure 4.** Influence of Gly228Arg substitution for the specific avian H3-avian  $\alpha$ -3 recognition: (A and B) model of maNY6874/78 H3-avian  $\alpha$ -2-3 complex; (C) model of dkHok8/80 H3-avian  $\alpha$ -2-3 complex (Gln226, Arg228, and Glu190 are not shown here). The models were prepared by an in silico substitution on the dkUkr/63-avian  $\alpha$ -2-3 complex.

basis of the follow argument. Employing the empirical entropic penalty of about  $1.5 \text{ cal mol}^{-1} \text{ K}^{-1}$  ( $0.5 \text{ kcal/mol}$  at  $298 \text{ K}$ ) per single rotatable bond,<sup>67,93–97</sup> avian Neu5Ac $\alpha$ -2-3Gal receptor can have about  $1 \text{ kcal/mol}$  penalty with two rotatable bonds on  $\alpha$ -2-3 linkage, and human Neu5Ac $\alpha$ -2-6Gal receptor can suffer about  $1.5 \text{ kcal/mol}$  penalty with three rotatable bonds on  $\alpha$ -2-6 linkage. Taking into account the nonspecific interaction (small

enthalpic contribution) of Gal residue on Neu5Ac $\alpha$ -2-6Gal, the torsional entropic penalty will be less than  $1.5 \text{ kcal/mol}$ . Vibrational entropic contribution on Gal residue is included in the total entropy  $T\Delta S_{\text{solute}}$ ; we did not explicitly break the total entropy into residue contributions.

**Origin of the Favorable Avian H3 Gln226Leu-Human  $\alpha$ -2-6 Binding.** The substitution of Gln226Leu in avian H3 HA1 enhances its affinity to human  $\alpha$ -2-6 (Table 1, entry 11). To understand the driving forces for this, we performed pair interaction energy decomposition analysis (PIEDA)<sup>64</sup> for the complexes, which decompose the total interaction energies into components. The dispersion interaction components are as follows: for human  $\alpha$ -2-6 and Leu226 in H3 Gln226Leu the value is  $-4.5 \text{ kcal/mol}$ , and for human  $\alpha$ -2-6 and Gln226 in H3 the value is  $-7.3 \text{ kcal/mol}$ . The preferential avian H3 Gln226Leu-human  $\alpha$ -2-6 binding in comparison with the negative avian H3-human  $\alpha$ -2-6 binding arises from the following two factors: (1) the intermolecular dispersion stabilization between Leu226 and human  $\alpha$ -2-6, and (2) a small  $T\Delta S_{\text{solute}}$  penalty.

The Gln226Leu substitution in the avian H3-sialoside complexes destroys the intermolecular hydrogen bonds between  $\text{H}_2\text{NOC-Gln226}$  and Neu5Ac  $1\text{-COO } 8\text{-OH}$  in both  $\alpha$ -2-3 and  $\alpha$ -2-6. The released  $1\text{-COO}$  forms an intramolecular hydrogen bond with  $8\text{-OH}$  to stabilize the complex, which is supported by neighboring intermolecular hydrogen bonds Neu5Ac  $8\text{-HO}\cdots\text{HO-Tyr98}$  and  $\text{H}^{\text{Ne}}\text{-His183}$ .<sup>58</sup> The  $1\text{-COO}\cdots\text{HO-8}$  interaction on Neu5Ac $\alpha$  was observed in the free state  $\alpha$ -sialoside in solution by the nuclear Overhauser effect,<sup>98</sup> whose stability was evaluated in the conformational study at the B3LYP/6-31++G(d,p)//B3LYP/6-31G(d,p) level.<sup>99</sup> Instead of breaking the Neu5Ac $\cdots$ Gln226 interaction by the substitution Gln226Leu, the *iso*-butyl group on Leu226 with its own hydrophobic backyard associates to Gal  $6\text{-CH}_2$  in human  $\alpha$ -2-6 by the dispersion stabilization.<sup>58</sup> This interaction change from the electrostatic Gln226 $\cdots$ human  $\alpha$ -2-6 to the Leu226 $\cdots$ human  $\alpha$ -2-6 dispersion provides a less favorable  $\Delta E_{\text{gas}}$  of  $+11.4 \text{ kcal/mol}$  (Table 1, entry 1 and Tables S7–S9) and a smaller  $\Delta G_{\text{es}}$  penalty of  $-8.3 \text{ kcal/mol}$  (entry 4).

The other  $\Delta G_{\text{solvation}}$  components are quite similar in both complexes (entries 2, 5–7), which indicates that the intermolecular interaction change between the Gln226 $\cdots$ human  $\alpha$ -2-6 hydrogen bond and Leu226 $\cdots$ human  $\alpha$ -2-6 association qualitatively constitutes the  $\Delta G_{\text{es}}$  difference. In terms of  $T\Delta S_{\text{solute}}$ , the above interaction change, consisting of the lost intermolecular hydrogen bond, the formed stable intramolecular hydrogen bond, and the loosened lipophilic association, gives a smaller penalty, leading to the more favorable  $\Delta G_{\text{bind},\alpha-2-6}$  (entries 10 and 11). Our results rationalize that the Gln226Leu substitution in dkUkr/1/63 H3 HA1 dramatically alters its binding specificity from avian  $\alpha$ -2-3 to human  $\alpha$ -2-6,<sup>32</sup> although to the best of our knowledge there are no titration data to compare with.

**Origin of the Remarkable Human H3-Human  $\alpha$ -2-6 Binding.** At the equilibrium, the intrinsic dissociation constant  $K_{\text{D}} = 2.1 \pm 0.3 \text{ mM}$  ( $\Delta G_{\text{bind}} = -3.7$  to  $-3.6 \text{ kcal/mol}$ ) under simple binding model for human H3 (X-31, Aichi2/68) in complex with Neu5Ac $\alpha$ -2-6Gal $\beta$ 1-4Glc was measured in the nuclear magnetic resonance titration study at  $297 \pm 1 \text{ K}$ .<sup>8</sup> The Neu5Ac $\alpha$ -2-6Gal $\beta$ 1-4Glc had  $K_{\text{D}} = 3.2 \text{ mM}$  ( $\Delta G_{\text{bind}} = -3.2$

(93) Pickett, S. D.; Sternberg, M. J. E. *J. Mol. Biol.* **1993**, *231*, 825–839.

(94) Wang, J.; Szewczuk, Z.; Yue, S.-Y.; Tsuda, Y.; Konishi, Y.; Purisima, E. O. *J. Mol. Biol.* **1995**, *253*, 473–492.

(95) Luo, R.; Gilson, M. K. *J. Am. Chem. Soc.* **2000**, *122*, 2934–2937.

(96) Lazaridis, T.; Masunov, A.; Gandolfo, F. *Proteins: Struct., Funct., Genet.* **2002**, *47*, 194–208.

(97) Chang, C. A.; Chen, W.; Gilson, M. K. *Proc. Natl. Acad. Sci. U.S.A.* **2007**, *104*, 1534–1539.

(98) Poppe, L.; Halbeek, H. V. *J. Am. Chem. Soc.* **1991**, *113*, 363–365.

(99) Sawada, T.; Hashimoto, T.; Shigematsu, M.; Ishida, H.; Kiso, M. *J. Carbohydr. Chem.* **2006**, *25*, 387–405.



kcal/mol) under the binding inhibition assay at 4 °C toward the association between solid phase-attached Aichi2/68 virion and peroxidase-labeled fetuin.<sup>100</sup> Our computational approach estimates that  $\Delta G_{\text{bind},\alpha 2-6}$  of X-31 H3 HA1 is  $-4.3$  kcal/mol (Table 1, entry 11). In comparison with the avian H3 Gln226Leu–human  $\alpha 2-6$  binding, the original human H3–human  $\alpha 2-6$  binding has a more favorable  $\Delta E_{\text{gas}}$  (entry 1) with a Leu226•••Gal dispersion stabilization (Table S10, entry 14), a larger  $\Delta G_{\text{solvation}}$  penalty (similar  $\Delta G_{\text{PCM}}$ , entries 8,9), and a smaller  $T\Delta S_{\text{solute}}$  penalty resulting in the exothermic  $\Delta G_{\text{bind},\alpha 2-6}$  (entry 10).

The component analysis of  $\Delta G_{\text{bind},\alpha 2-6}$  difference clarifies the chemical aspects of the remarkable human H3–human  $\alpha 2-6$  binding. Here we make suggestion 1, the remarkable human H3–human  $\alpha 2-6$  binding does not originate from the intermolecular hydrogen-bond formation between Ser228-OH and OH-9 Neu5Ac; and suggestion 2, the hydrophilic recognition of 1-COO on Neu5Ac residue by Ser136, Asn137, and Ser145 is necessary for the human H3 (Aichi2/68)–human  $\alpha 2-6$  binding, but this intermolecular hydrogen-bond network is not sufficient for the striking human H3–human  $\alpha 2-6$  binding.

According to the  $\Delta E_{\text{gas}}$  components comparison shown in Figure 2B, the additional hydrogen bond Ser228-OH•••OH-9 Neu5Ac stabilizes the human H3–human  $\alpha 2-6$  complex stronger than the Gly228•••OH-9 Neu5Ac interaction in the avian H3 Gln226Leu–human  $\alpha 2-6$  complex (Table S10, entry 13). But the intermolecular hydrogen-bond formation suffers a larger desolvation penalty, giving a  $\Delta G_{\text{PCM}}$  similar to that in the avian H3 Gln226Leu–human  $\alpha 2-6$  complex (Table 1, entry 9). Even if the favorable Ser228-OH•••OH-9 Neu5Ac interaction disappears, the other two hydrogen bonds Glu190-COO•••HO-9 Neu5Ac and His183-N<sup>H</sup>•••OH-9 Neu5Ac compensate the stability loss. In terms of the solute entropic change on the sialoside binding site, the intermolecular Ser228-OH•••OH-9 Neu5Ac hydrogen bond locally suffers a small vibrational entropy loss because the Ser228-OH forms the intramolecular hydrogen bond with OOC-Glu190 in the isolated human H3 HA1 before the complex formation.

Consequently, we conclude that the Ser228-OH•••OH-9 Neu5Ac interaction does not contribute to the remarkable human H3–human  $\alpha 2-6$  binding so much. This suggestion is consistent with the previous experimental data. The substitution of Ser228Gly on human H3 HA1 (X-31) retained the larger human H3–human erythrocyte binding affinity.<sup>101</sup> Methyl 9-deoxy- $\alpha$ -Neu5Ac inhibited the binding between the X-31 virus and Neu5Ac $\alpha 2-6$ Gal $\beta 1-4$ GlcNAc attached erythrocyte as much as methyl  $\alpha$ -Neu5Ac.<sup>102</sup> Methyl 9-amino-9-deoxy- $\alpha$ -Neu5Ac had no binding affinity to the bromelain-released X-31 human H3.<sup>9</sup> A/Udorn/307/1972 (H3N2, Udorn307/72) variant had two substitutions Leu226Gln and Ser228Gly on HA1 that quite weakly associated Neu5Ac $\alpha 2-6$ Gal $\beta 1-4$ GlcNAc $\beta$  bound polyacrylamide as much as the Udorn307/72 Leu226Gln variant;<sup>29</sup> in other words, the additional Ser228Gly substitution did not change critically the H3–human  $\alpha 2-6$  binding affinity. These discussions apply to old human H3N2 strains isolated prior to 1990 because the old human H3 HA1s keep Tyr98, His183, and Glu190 with the compensation capability toward losing the

Ser228-OH•••OH-9 Neu5Ac hydrogen bond. A similar compensation was confirmed in the Glu190Ala substitution on Aichi2/68 H3 HA1 but not in His183Phe.<sup>101</sup> Unfortunately, recent human H3N2 strains have Asp190 instead of Glu,<sup>22,103</sup> and their compensation capabilities to human  $\alpha 2-6$  affinity are not clear yet.

Next, we address the issue of the wide-range hydrophilic recognition (suggestion 2 in beginning of this section). Comparing the recognition of 1-COO Neu5Ac in human  $\alpha 2-6$  by human H3 and avian H3 Gln226Leu (Figure 2B), one can see that the human H3–human  $\alpha 2-6$  interaction has a binding advantage in the gas phase: a larger intermolecular PIE stability (Table S10, summation of entries 4–6, the 1-COO recognition is shown in Figure 3), a preferential intramolecular  $\Delta\Delta\text{PIE}$  (Table S11, see Ser136, Asn137, and Ser145), and a similar internal energy change (Table S12, the sum of entries 4–6 and 15). But this advantage is compensated by a larger desolvation penalty giving a  $\Delta G_{\text{PCM}}$  similar to that in the avian H3 Gln226Leu–human  $\alpha 2-6$  complex (Table 1, entry 9).

Thus, in Aichi2/68 H3 HA1, we make further suggestion 2-a, the human H3–human  $\alpha 2-6$  binding requires the intermolecular hydrogen-bond network between 1-COO Neu5Ac and amino acids 136, 137, and 145; suggestion 2-b, but this interaction does not contribute sufficiently to the distinctive human H3–human  $\alpha 2-6$  binding; and suggestion 2-c, the above two suggestions admit that possible amino acid substitutions may optimize the recognition for 1-COO Neu5Ac to accelerate the strong human H3–human  $\alpha 2-6$  binding. Here, we do not consider the solute entropic effect on the intermolecular hydrogen-bond network around 1-COO Neu5Ac because of the decomposition analysis difficulty. Probably the entropic effect would influence the adjacent intermolecular hydrophobic association between Leu226 and 6-CH<sub>2</sub> Gal in human  $\alpha 2-6$ .

The suggestion 2-a qualitatively explains the reported human H3N2 binding to human  $\alpha 2-6$ . The substitution Ser136Ala in human H3 HA1 (X-31) decreased its binding affinity to human erythrocyte due to the loss of the intermolecular hydrogen bond Ser136-OH•••OOC1-Neu5Ac.<sup>101</sup> The substitution Ser136Thr also decreased the human erythrocyte binding, but its affinity was slightly larger than human H3 Ser136Ala.<sup>101</sup> The Thr136 could form the Thr136-OH•••OOC1-Neu5Ac hydrogen bond with a similarity to the original Ser136-OH•••OOC1-Neu5Ac. However, the Ser136Thr substitution caused a larger steric hindrance, resulting in a change in the interaction between Asn137, Ser145, and outside 1-COO Neu5Ac. Besides, the steric repulsion in Thr136 might prevent its backbone hydrogen-bond formations Thr136-NH•••OC-Gly146 and Ala138-NH•••OC-Thr136. We note that these discussions pertain to known H3 HA1–sialoside binding, not to H1 subtype.<sup>27,104</sup>

The amino acid sequence analysis of known human H3 HA1s supports indirectly the suggestions 2-b and 2-c. On the sequence alignment for avian and human H3s since 1963, the Ser136 preservation is significant for the recognition of 1-COO Neu5Ac regardless of their binding specificities.<sup>29</sup> Additional experimental evidence is that one-point substitutions Ser136Cys and

(100) Matrosovich, M. N.; Gambaryan, A. S.; Tuzikov, A. B.; Byramova, N. E.; Mochalova, L. V.; Golbraikh, A. A.; Shenderovich, M. D.; Finne, J.; Bovin, N. V. *Virology* **1993**, *196*, 111–121.

(101) Martin, J.; Wharton, S. A.; Lin, Y. P.; Takemoto, D. K.; Skehel, J. J.; Wiley, D. C.; Steinhauer, D. A. *Virology* **1998**, *241*, 101–111.

(102) Kelm, S.; Paulson, J. C.; Rose, U.; Brossmer, R. R.; Schmid, W.; Bandgar, B. P.; Schreiner, E.; Hartmann, M.; Zbiral, E. *Eur. J. Biochem.* **1992**, *205*, 147–153.

(103) Nobusawa, E.; Ishihara, H.; Morishita, T.; Sato, K.; Nakajima, K. *Virology* **2000**, *278*, 587–596.

(104) Watowich, S. J.; Skehel, J. J.; Wiley, D. C. *Structure* **1994**, *2*, 719–731.

**Table 2.** Transition of the Cooperative Interaction to 1-COO Neu5Ac and the  $\alpha$ -2-6 Glycosyl Bond in Human  $\alpha$ -2-6

amino acid position <sup>a</sup>				human A virus H3N2 strains <sup>b</sup>
136	137	145	226	
Ser	Asn	Ser	Leu	Hong Kong/1/1968, Aichi/2/1968, Memphis/1/1971, Memphis/102/1972, Udorn/307/1972, Port Chalmers/1/1973, Tokyo/6/1973
Ser	Ser	Ser	Leu	Victoria/3/1975
Ser	Ser	Asn	Leu	Kumamoto/55/1976, Yamanashi/2/1977
Ser	Tyr	Asn	Leu	Texas/1/1977, Los Angeles/2/1987, Memphis/8/1988, England/427/1988, Shanghai/11/1989, Tottori/894/1994
Ser	Tyr	Lys	Leu	Bangkok/1/1979, Philippines/2/1982, Philippines/2/1982 X-79, NIB/3/90E (England/427/1988 variant)
Ser	Tyr	Lys	Val	Paris/1997, Switzerland/7729/1998
Ser	Ser	Lys	Val	Memphis/31/1998, Hong Kong/1180/1999
Ser	Ser	Asn	Ile	Oklahoma/323/2003, Oklahoma/369/2005

<sup>a</sup> Some information was taken from Genbank in the National Center for Biotechnology Information databases. <sup>b</sup> References are listed in SI Appendix S4.

Ser136Asn in the human H3 HA1s of Aichi2/68 and A/Sydney/5/1997 lost their hemadsorption activities to human red blood cells.<sup>105,106</sup>

On the other hand, the substitutions at position 137 and 145 took place, maintaining or increasing the preferential human H3–human  $\alpha$ -2-6 binding. The reported human H3 strains in Table 2 (references are listed in Supporting Information Appendix S4) experimentally proved the favorable Neu5Ac $\alpha$ -2-6Gal affinities and HA1 amino acid sequence. The exchange between Asn and Ser at positions 137 and 145 almost retained the recognition of 1-COO Neu5Ac in human  $\alpha$ -2-6 (Figure 3). At the position 145, hydrophilic side-chains with a suitable length on Asn and Lys easily interact with the outer edge in the 1-COO Neu5Ac moiety. The Asn/Lys145 side-chain $\cdots$ OOC-1 Neu5Ac interaction did not always require an aid from the hydrophilic amino acid at 137. Asn145 and Lys145 sometimes required a hydrophobic Tyr and Phe at position 137 (Phe was observed in A/Tokyo/1998 H3 HA1<sup>107</sup>). The *p*-hydroxyphenyl group on Tyr137 might interact with the out-edge in human  $\alpha$ -2-6, the stabilization by Tyr137-aromatic  $\pi\cdots$ CH<sub>2</sub>-3/HO-4 Neu5Ac interactions and hydrogen-bond formation of Tyr137-OH $\cdots$ O-6 Gal. The Tyr137 $\cdots$ human  $\alpha$ -2-6 interaction probably cooperated with the hydrophobic Leu226 (or Val, Ile) $\cdots$ human  $\alpha$ -2-6 association, leading to a larger entropic advantage.

**Prospects for Monovalent Inhibitor to Human H3 and Avian H3 Gln226Leu–Human  $\alpha$ -2-6 Binding.** In the 1980–1990s, a number of monovalent sialoside derivatives with various hydrophobic aglycons were investigated to design a strong monovalent inhibitor to the Aichi2/68 H3–cell surface sialoside association.<sup>10,100,102,104,108</sup> Weinhold and Knowles synthesized 4-*O*-dansylglycyl- $\alpha$ -Neu5Ac derivative with a glycon part [6-(((naphthylmethyl)amino)carbonyl)hexyl], which had  $K_D = 3.7 \pm 0.6 \mu\text{M}$  to the bromelain-released H3 (X-31, Aichi2/68).<sup>10</sup> Following the above result, Watowich et al. discussed that the high-affinity reflected suitable intermolecular hydrogen-bond formations and hydrophobic energy contributions via buried apolar solvent accessible surface.<sup>104</sup>

FMO/PCM predicts the strong intermolecular dispersion stabilization of Leu226 and lipophilic site on Gal residue. This

is significant for the binding between human H3/avian H3 Gln226Leu and  $\alpha$ -sialoside derivatives, which are used as potential drugs for treatment of influenza. In these sialoside derivatives, an elaborate aglycon component is added to the inhibitor, and the choice of such aglycon addition manipulates the efficiency of such drugs. Generally, the intermolecular dispersion depends on molecular polarizability, for example, nonpolar H<sub>3</sub>C–CH<sub>3</sub> versus polar H<sub>3</sub>C <sup>$\delta^+$</sup> – $\delta^-$ -Cl, shape of molecule, for example, *n*-butyl versus *tert*-butyl, and the atomic composition with more electrons, for example, CH<sub>3</sub>–CH<sub>2</sub>–CH<sub>3</sub> versus CH<sub>3</sub>–S–CH<sub>3</sub>. Thus, one can suggest the aglycon conversion from –CH<sub>2</sub>– group to polarizable –C(H)– or –CFH– groups, from a linear aliphatic chain –CH<sub>2</sub>–CH<sub>2</sub>–CH<sub>2</sub>–CH<sub>2</sub>– to branched chain –CH(CH<sub>2</sub>–CH<sub>3</sub>)–CH<sub>2</sub>– as plausible alternations in the inhibitor structure. To avoid the hydrolysis of the Neu5Ac $\alpha$ -aglycon bond caused by viral neuraminidase, the –CFH– moiety as an electron-withdrawing group can be put adjacent to the glycoside bond.<sup>109,110</sup>

The fact that the polyvalent sialoside receptor strongly binds to viral HA motivates us to design polyvalent sialoglycoconjugates as an inhibitor for the virion–sialoside receptor association. However, these conjugates are not suitable as a drug due to their large molecular sizes. One of the approaches to inhibit the HA–sialoside association without polyvalent sialoglycoconjugate is a selective chemical ligation<sup>111–113</sup> between HA and sialoside derivative. The sialoside derivative requires a sialoside moiety, a reactive group to form a selective covalent bond with amino acid residues side-chains (nucleophile) on HA under mild condition, and a suitable linker between the sialoside moiety and the reactive group. In this approach, the HA–inhibitor encounter phase can be controlled by the intramolecular interaction to achieve small  $K_D$  on the HA–inhibitor complex, very fast association rate and moderate dissociation rate on the intramolecular HA–inhibitor binding.

## Conclusions

The FMO-MP2/PCM method with the molecular mechanics level estimate of the solute entropy change has qualitatively

- (105) Nakajima, K.; Nobusawa, E.; Tonegawa, K.; Nakajima, S. *J. Virol.* **2003**, *77*, 10088–10098.  
 (106) Nakajima, K.; Nobusawa, E.; Nagy, A.; Nakajima, S. *J. Virol.* **2005**, *79*, 6472–6477.  
 (107) Mori, S.-I.; Nagashima, M.; Sasaki, Y.; Mori, K.; Tabei, Y.; Yoshida, Y.; Yamazaki, K.; Hirata, I.; Sekine, H.; Ito, T.; Suzuki, S. *Arch. Virol.* **1999**, *144*, 147–155.  
 (108) Toogood, P. L.; Galliker, P. K.; Glick, G. D.; Knowles, J. R. *J. Med. Chem.* **1991**, *34*, 3138–3140.

- (109) Sun, X.-L.; Kanie, Y.; Guo, C.-T.; Kanie, O.; Suzuki, Y.; Wong, C.-H. *Eur. J. Org. Chem.* **2000**, *14*, 2643–2653.  
 (110) Buchini, S.; Buschiazzo, A.; Withers, S. G. *Angew. Chem., Int. Ed.* **2008**, *47*, 2700–2703.  
 (111) Takaya, K.; Nagahori, N.; Kuroguchi, M.; Furuie, T.; Miura, N.; Monde, K.; Lee, Y. C.; Nishimura, S.-I. *J. Med. Chem.* **2005**, *48*, 6054–6065.  
 (112) Evans, M. J.; Cravatt, B. F. *Chem. Rev.* **2006**, *106*, 3279–3301.  
 (113) Tsukiji, S.; Miyagawa, M.; Takaoka, Y.; Tamura, T.; Hamachi, I. *Nat. Chem. Biol.* **2009**, *5*, 341–343.

rationalized the specific binding of avian and human H3 HA1s to  $\alpha$ -sialosides. Our  $\Delta G_{\text{bind}}$  component analysis has revealed the role of key mutation in the selective H3–sialoside interaction. In this work, we have proved the validity of the physical interpretation by a very detailed comparison to various experimental data, while we suggest that qualitative or semiquantitative agreement has been achieved.

The strong avian H3 (dkUkr/63)–avian Neu5Ac $\alpha$ 2-3Gal binding arises from the hydrogen-bond interaction between the 4-OH group on Gal and the side-chain on the Gln226 residue under the hydrogen-bond network formation between the 1-COO group on Neu5Ac moiety, amino acid residues at 136, 137, and 145. The reason a substitution Gln226Leu in avian H3 HA1 increases the binding affinity to human Neu5Ac $\alpha$ 2-6Gal is the Leu226 $\cdots$ human  $\alpha$ 2-6 dispersion interaction with a small entropic penalty. The remarkable human H3–human Neu5Ac $\alpha$ 2-6Gal binding is not governed by the Ser228-OH $\cdots$ OH-9 Neu5Ac hydrogen bond. The Aichi2/68 H3 binding to human  $\alpha$ 2-6 requires the hydrophilic recognition of 1-COO on Neu5Ac residue by Ser136, Asn137, Ser145, but this interaction is not sufficient for the striking human  $\alpha$ 2-6 binding. Therefore, possible amino acid substitutions optimize the recognition of 1-COO Neu5Ac and  $\alpha$ 2-6 bond to accelerate the strong human H3–human  $\alpha$ 2-6 binding. These chemical aspects can be valuable in designing monovalent inhibitors of influenza viral HA–sialoside binding, and they can help us in understanding the binding of various viral HAs and their mutants.

**Acknowledgment.** This work was supported by contract grant sponsors: CREST (JST, Japan) and The Next Generation Super

Computing Project and Nanoscience Program (MEXT, Japan). We would like to thank Dr. Yuri Alexeev for many fruitful discussions.

**Note Added after ASAP Publication.** This article was published on November 4, 2010. A correction was made to the  $\Delta G_{\text{bind}}$  equation in the Estimation of Binding Free Energies section. The corrected version was reposted on November 10, 2010.

**Supporting Information Available:** Amino acid sequences and secondary structures of avian and human H3 HA1 domains (Table S1), definitions for the dihedral angles of the  $\alpha$ 2-6 bond on Neu5Ac $\alpha$ 2-6Gal (Figure S1), validity of the energy-minimized H3 HA1–Neu5Ac $\alpha$ 2-3 and  $\alpha$ 2-6Gal complexes toward the  $\Delta G_{\text{bind}}$  estimations (Appendix S1, Table S2, and Figures S2–S5), weakly constrained H<sub>2</sub>O in the molecular dynamics (MD) simulations of H3 HA1s in complex with Neu5Ac $\alpha$ 2-3 and  $\alpha$ 2-6Gal $\beta$ 1-4Glc (Appendix S2, Figures S6–S8), details of the FMO/PCM setup and fragmentation of the models (Appendix S3, Figures S9 and S10, and Table S3), details of  $\Delta\Delta E_{\text{gas}}$  between the avian H3–avian  $\alpha$ 2-3 complex and avian H3–human  $\alpha$ 2-6 complex (Tables S4–S6), between avian H3 Gln226Leu–human  $\alpha$ 2-6 complex and avian H3–human  $\alpha$ 2-6 complex (Tables S7–S9), between human H3–human  $\alpha$ 2-6 complex and avian H3 Gln226Leu–human  $\alpha$ 2-6 complex (Tables S10–S12), and the reported preferential human H3 strains–human  $\alpha$ 2-6 binding and their amino acid sequences (Appendix S4). This material is available free of charge via the Internet at <http://pubs.acs.org>.

JA105051E